

RESEARCH ARTICLE

Logic Bell state concentration with parity check measurement

Jiu Liu¹, Lan Zhou², Wei Zhong¹, Yu-Bo Sheng^{1,3,†}

¹*Institute of Quantum Information and Technology, Nanjing University of Posts and Telecommunications, Nanjing 210003, China*

²*School of Science, Nanjing University of Posts and Telecommunications, Nanjing 210003, China*

³*Key Lab of Broadband Wireless Communication and Sensor Network Technology (Ministry of Education), Nanjing University of Posts and Telecommunications, Nanjing 210003, China*

Corresponding author. E-mail: †shengyb@njupt.edu.cn

Received July 21, 2018; accepted September 27, 2018

Logic qubit plays an important role in current quantum communication. In this paper, we propose an efficient entanglement concentration protocol (ECP) for a new kind of logic Bell state, where the logic qubit is the concatenated Greenber–Horne–Zeilinger (C-GHZ) state. Our ECP relies on the nondemolition polarization parity check (PPC) gates constructed with cross-Kerr nonlinearity, and can distill one pair of maximally entangled logic Bell state from two same pairs of less-entangled logic Bell states. Benefit from the nondemolition PPC gates, the concentrated maximally entangled logic Bell state can be remained for further application. Moreover, our ECP can be repeated to further concentrate the less-entangled logic Bell state. By repeating the ECP, the total success probability can be effectively increased. Based on above features, this ECP may be useful in future long-distance quantum communication.

Keywords concatenated Greenber–Horne–Zeilinger (C-GHZ) state, single photon, cross-Kerr nonlinearity

1 Introduction

In recent years, quantum information technology has made many exciting progresses both in theory and experiment. Comparing with classic information technology, quantum information technology shows attractive advantages, such as the absolute security. Quantum entanglement is an important source in many fields of quantum information technology, such as quantum computation [1], quantum teleportation [2–5], quantum key distribution [6, 7], quantum secure direct communication [8–13], quantum machine learning [14], and so on [15–23]. However, in the actual quantum information processing, the entangled particles will inevitably interact with the external noisy environment, which may result in the decoherence. The decoherence may cause negative impact on the applications of entanglement. For example, in the practical applications in quantum communication field, a degraded entanglement channel may degrade the fidelity of the teleportation, even more, it will make the quantum communication insecure. Therefore, we should recover the degraded entangled state into the maximally entangled state. In quantum communication, the methods to solve the decoherence problem are called entanglement purification and entanglement concentration.

Entanglement purification is to distill some pairs of particles in highly entangled states from a set of mixed states [24–30]. Entanglement concentration, which will be de-

tailed here, is used to recover the less-entangled states into the maximally entangled ones [31–43]. In 1996, Bennett *et al.* proposed the concept of entanglement concentration and contrived the first entanglement concentration protocol (ECP) [31], which based on Schmidt decomposition. Subsequently, many efficient ECPs have been proposed. Existing ECPs usually can be divided into two groups. The ECPs in the first group can concentrate the less-entangled states encoded in the physical qubits directly, including the ECPs for photonic polarization entanglement, the spin in quantum-dot and optical microcavities, atomic entanglement, the nitrogen-vacancy center and microresonator systems, and so on [32–41]. The ECPs in the second group focus on the logic-qubit entanglement concentration [42, 43]. Logic qubit entanglement, which encodes many physical qubits in a logic qubit, is widely used in quantum computation [44, 45]. In 2011, Fröwis and Dür first proposed a kind of logic-qubit entanglement, i.e., the concatenated Greenberger–Horne–Zeilinger (C-GHZ) state [46], which was later experimentally realized by Lu *et al.* in linear optics [47]. They also showed that the C-GHZ state is useful for large-scale fiber-based quantum networks and multipartite QKD, QSS and third-man quantum cryptography [47]. The C-GHZ state has the form of [46–53]

$$|\Psi\rangle_{C-GHZ} = \frac{1}{\sqrt{2}}(|GHZ_m^+\rangle^{\otimes n} + |GHZ_m^-\rangle^{\otimes n}), \quad (1)$$

where

$$|GHZ_m^\pm\rangle = \frac{1}{\sqrt{2}}(|0\rangle^{\otimes m} \pm |1\rangle^{\otimes m}). \quad (2)$$

Here, n is the number of logic qubits, and m is the number of physical qubits in each logic qubit. In 2015, with the help of the controlled-not gate (C-NOT gate), Qu *et al.* proposed an ECP for the C-GHZ state [42]. Subsequently, Pan *et al.* proposed a linear optical ECP for the C-GHZ state [43].

In this paper, we will research on a linear optical ECP for a new kind of logic Bell state with the help of polarization parity check (PPC) measurement. In our logic Bell state, each logic qubit is encoded in a C-GHZ state. We define logic qubit $|\bar{0}\rangle$ as $|0\rangle^{(n,m)} = \frac{1}{\sqrt{2}}(|GHZ_m^+\rangle^{\otimes n} + |GHZ_m^-\rangle^{\otimes n})$, and $|\bar{1}\rangle$ as $|1\rangle^{(n,m)} = \frac{1}{\sqrt{2}}(|GHZ_m^+\rangle^{\otimes n} - |GHZ_m^-\rangle^{\otimes n})$, respectively. Such logic qubit is also called the quantum parity code [54–56] and it has the advantage of incorporating protection against transmission losses. Therefore, the logic Bell state has application potential in ultrafast high-rate long-distance quantum communication [57, 58].

This paper is organized as follows. In Section 2, we first introduce the structure of the logic Bell state and the PPC measurement. In Section 3, we explain our ECP for the logic Bell state. We first describe this ECP for the simple cases of $m = n = 2$ and $m = 2, n = 3$, respectively. Then we extend the ECP to the logic Bell state with arbitrary m and n . In Section 4, we provide some discussion. In Section 5, we give a conclusion.

2 The structure of the logic Bell state and the PPC measurement

In this section, we first briefly show the structure of the logic Bell state in an optical polarization system. We denote $|H\rangle$ as $|0\rangle$ and $|V\rangle$ as $|1\rangle$. $|H\rangle$ and $|V\rangle$ mean the horizontal and vertical polarization of the photon qubit, respectively. The logic qubit in the logic Bell state is defined as

$$\begin{aligned} |\bar{H}\rangle^{(n,m)} &= \frac{1}{\sqrt{2}}(|GHZ_m^+\rangle^{\otimes n} + |GHZ_m^-\rangle^{\otimes n}), \\ |\bar{V}\rangle^{(n,m)} &= \frac{1}{\sqrt{2}}(|GHZ_m^+\rangle^{\otimes n} - |GHZ_m^-\rangle^{\otimes n}), \end{aligned} \quad (3)$$

where

$$|GHZ_m^\pm\rangle = \frac{1}{\sqrt{2}}(|H\rangle^{\otimes m} \pm |V\rangle^{\otimes m}). \quad (4)$$

The less-entangled logic Bell state can be written as

$$|\varphi\rangle^{(n,m)} = \alpha|\bar{H}\rangle^{(n,m)}|\bar{H}\rangle^{(n,m)} + \beta|\bar{V}\rangle^{(n,m)}|\bar{V}\rangle^{(n,m)}, \quad (5)$$

where $|\alpha|^2 + |\beta|^2 = 1$. If $m = n = 1$, it simplifies to the standard Bell-state.

The PPC measurement in our paper essentially acts as the role of quantum nondemolition detector (QND), whose basic principle is shown in Fig. 1. The PPC measurement can be implemented with cross-Kerr nonlinear-

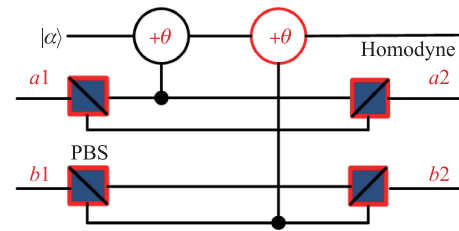


Fig. 1 The schematic drawing of the polarization parity check (PPC) measurement [59]. PBS represents the polarization beam splitter, which can transmit the photon in $|H\rangle$ and reflect the photon in $|V\rangle$. It can be found that both the photon of $|H\rangle$ in the spatial mode $a1$ and the photon of $|V\rangle$ in the spatial mode $b1$ will make the coherent state pick up the phase shift of θ .

ity [59], which is a powerful tool in quantum information processing [59–65].

Next, we will introduce the working principle of QND. In Fig. 1, we let a photon in the state of $|\Pi_1\rangle = \mu|H\rangle_{a1} + \nu|V\rangle_{a1}$ and a photon in $|\Pi_2\rangle = \gamma|H\rangle_{b1} + \delta|V\rangle_{b1}$ pass through the QND, where $|\mu|^2 + |\nu|^2 = 1$ and $|\gamma|^2 + |\delta|^2 = 1$. After the QND, the two-photon state combined with the coherent state $|\alpha\rangle$ will evolve to

$$\begin{aligned} |\Pi_1\rangle \otimes |\Pi_2\rangle \otimes |\alpha\rangle &\rightarrow (\mu\gamma|H\rangle_{a1}|H\rangle_{b1} + \nu\delta|V\rangle_{a1}|V\rangle_{b1})|\alpha e^{i\theta}\rangle \\ &\quad + \mu\delta|H\rangle_{a1}|V\rangle_{b1}|\alpha e^{i2\theta}\rangle + \nu\gamma|V\rangle_{a1}|H\rangle_{b1}|\alpha\rangle. \end{aligned} \quad (6)$$

From Eq. (6), the odd (O) parity items $|H\rangle_{a1}|V\rangle_{b1}$ and $|V\rangle_{a1}|H\rangle_{b1}$ make the coherence state $|\alpha\rangle$ shift with 2θ and 0 , respectively, while the even (E) parity states $|H\rangle_{a1}|H\rangle_{b1}$ and $|V\rangle_{a1}|V\rangle_{b1}$ both make $|\alpha\rangle$ shift with θ . If we set θ equal to π , the shifts 0 and 2θ will not be distinguished. As a result, this two-photon system can be divided into two classes, one corresponds to the shift of θ on the coherence state $|\alpha\rangle$, the other one corresponds to the phase shift of 0 (2θ). Consequently, we can carry out a polarization parity check (PPC) measurement by detecting the phase shift of the coherent state without destroying the photons. If the detection result is θ , it means that the initial state in Eq. (6) will collapse to the E parity item $|H\rangle|H\rangle$ or $|V\rangle|V\rangle$. If the detection result 0 (2θ), it means the state in Eq. (6) will collapse to the O parity item $|H\rangle|V\rangle$ or $|V\rangle|H\rangle$.

3 The entanglement concentration protocol for the logic Bell state

The aim of our ECP is to distill the maximally entangled logic Bell state from the less-entangled logic Bell state in Eq. (5). The maximally entangled logic Bell state can be written as

$$|\Theta\rangle^{(n,m)} = \frac{1}{\sqrt{2}}(|\bar{H}\rangle^{(n,m)}|\bar{H}\rangle^{(n,m)} + |\bar{V}\rangle^{(n,m)}|\bar{V}\rangle^{(n,m)}). \quad (7)$$

Firstly, we let $m = n = 2$ to show the basic principle of this ECP. The schematic drawing of the ECP is shown in

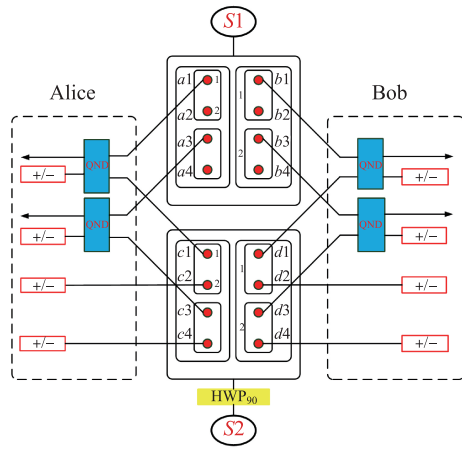


Fig. 2 The schematic drawing of the ECP under the case of $m = n = 2$. $S1$ and $S2$ are two sources of less-entangled logic Bell state. The two big boxes represent two logic Bell states. Two moderate boxes in each big box represent the two C-GHZ states in each logic Bell state. The number of the small boxes in each moderate box equals to n . The red dot in the small box represents the photonic physical qubit. The number of red dots in each small box equals to m . HWP is a half-wave plate which can make $|H\rangle \leftrightarrow |V\rangle$. The QND whose structure is shown in FIG. 1, is to make a polarization parity check (PPC) measurement. The “+/-” in the red long box indicates measurement under basis of $|\pm\rangle = \frac{1}{\sqrt{2}}(|H\rangle \pm |V\rangle)$.

Fig. 2. Our ECP needs two pairs of identical less-entangled logic Bell states, named $|\bar{\phi}_1\rangle^{(2,2)}$ and $|\bar{\phi}_2\rangle^{(2,2)}$ with the form of

$$\begin{aligned}
 &|\bar{\phi}_1\rangle^{(2,2)} \\
 &= \alpha|\bar{H}\rangle_a^{(2,2)}|\bar{H}\rangle_b^{(2,2)} + \beta|\bar{V}\rangle_a^{(2,2)}|\bar{V}\rangle_b^{(2,2)} \\
 &= \alpha\left[\frac{1}{\sqrt{2}}(|H\rangle_{a1}|H\rangle_{a2}|H\rangle_{a3}|H\rangle_{a4} + |V\rangle_{a1}|V\rangle_{a2}|V\rangle_{a3}|V\rangle_{a4})\right. \\
 &\quad \left.\frac{1}{\sqrt{2}}(|H\rangle_{b1}|H\rangle_{b2}|H\rangle_{b3}|H\rangle_{b4} + |V\rangle_{b1}|V\rangle_{b2}|V\rangle_{b3}|V\rangle_{b4})\right] \\
 &+ \beta\left[\frac{1}{\sqrt{2}}(|H\rangle_{a1}|H\rangle_{a2}|V\rangle_{a3}|V\rangle_{a4} + |V\rangle_{a1}|V\rangle_{a2}|H\rangle_{a3}|H\rangle_{a4})\right. \\
 &\quad \left.\frac{1}{\sqrt{2}}(|H\rangle_{b1}|H\rangle_{b2}|V\rangle_{b3}|V\rangle_{b4} + |V\rangle_{b1}|V\rangle_{b2}|H\rangle_{b3}|H\rangle_{b4})\right], \quad (8)
 \end{aligned}$$

$$\begin{aligned}
 &|\bar{\phi}_2\rangle^{(2,2)} \\
 &= \alpha|\bar{H}\rangle_c^{(2,2)}|\bar{H}\rangle_d^{(2,2)} + \beta|\bar{V}\rangle_c^{(2,2)}|\bar{V}\rangle_d^{(2,2)} \\
 &= \alpha\left[\frac{1}{\sqrt{2}}(|H\rangle_{c1}|H\rangle_{c2}|H\rangle_{c3}|H\rangle_{c4} + |V\rangle_{c1}|V\rangle_{c2}|V\rangle_{c3}|V\rangle_{c4})\right. \\
 &\quad \left.\frac{1}{\sqrt{2}}(|H\rangle_{d1}|H\rangle_{d2}|H\rangle_{d3}|H\rangle_{d4} + |V\rangle_{d1}|V\rangle_{d2}|V\rangle_{d3}|V\rangle_{d4})\right] \\
 &+ \beta\left[\frac{1}{\sqrt{2}}(|H\rangle_{c1}|H\rangle_{c2}|V\rangle_{c3}|V\rangle_{c4} + |V\rangle_{c1}|V\rangle_{c2}|H\rangle_{c3}|H\rangle_{c4})\right. \\
 &\quad \left.\frac{1}{\sqrt{2}}(|H\rangle_{d1}|H\rangle_{d2}|V\rangle_{d3}|V\rangle_{d4} + |V\rangle_{d1}|V\rangle_{d2}|H\rangle_{d3}|H\rangle_{d4})\right]. \quad (9)
 \end{aligned}$$

In Fig. 2, photons in the spatial modes $a1 - a4$ and $c1 - c4$ belong to Alice and the photons in the modes $b1 - b4$ and $d1 - d4$ belong to Bob. Firstly, Alice and

Bob both perform the bit-flip operations on the photons in modes $c1 - c4$ and $d1 - d4$ with the help of the half-wave plate (HWP), respectively. After that, $|\bar{\phi}_2\rangle^{(2,2)}$ can be converted to $|\bar{\phi}_3\rangle^{(2,2)}$ as

$$\begin{aligned}
 &|\bar{\phi}_3\rangle^{(2,2)} \\
 &= \beta|\bar{H}\rangle_c^{(2,2)}|\bar{H}\rangle_d^{(2,2)} + \alpha|\bar{V}\rangle_c^{(2,2)}|\bar{V}\rangle_d^{(2,2)} \\
 &= \beta\left[\frac{1}{\sqrt{2}}(|H\rangle_{c1}|H\rangle_{c2}|H\rangle_{c3}|H\rangle_{c4} + |V\rangle_{c1}|V\rangle_{c2}|V\rangle_{c3}|V\rangle_{c4})\right. \\
 &\quad \left.\frac{1}{\sqrt{2}}(|H\rangle_{d1}|H\rangle_{d2}|H\rangle_{d3}|H\rangle_{d4} + |V\rangle_{d1}|V\rangle_{d2}|V\rangle_{d3}|V\rangle_{d4})\right] \\
 &+ \alpha\left[\frac{1}{\sqrt{2}}(|H\rangle_{c1}|H\rangle_{c2}|V\rangle_{c3}|V\rangle_{c4} + |V\rangle_{c1}|V\rangle_{c2}|H\rangle_{c3}|H\rangle_{c4})\right. \\
 &\quad \left.\frac{1}{\sqrt{2}}(|H\rangle_{d1}|H\rangle_{d2}|V\rangle_{d3}|V\rangle_{d4} + |V\rangle_{d1}|V\rangle_{d2}|H\rangle_{d3}|H\rangle_{d4})\right]. \quad (10)
 \end{aligned}$$

In this way, the whole system can be described as

$$\begin{aligned}
 |\Phi\rangle = &\frac{\alpha\beta}{4}[(|H\rangle_{a1}|H\rangle_{a2}|H\rangle_{a3}|H\rangle_{a4} + |V\rangle_{a1}|V\rangle_{a2}|V\rangle_{a3}|V\rangle_{a4}) \\
 &(|H\rangle_{b1}|H\rangle_{b2}|H\rangle_{b3}|H\rangle_{b4} + |V\rangle_{b1}|V\rangle_{b2}|V\rangle_{b3}|V\rangle_{b4}) \\
 &(|H\rangle_{c1}|H\rangle_{c2}|H\rangle_{c3}|H\rangle_{c4} + |V\rangle_{c1}|V\rangle_{c2}|V\rangle_{c3}|V\rangle_{c4}) \\
 &(|H\rangle_{d1}|H\rangle_{d2}|H\rangle_{d3}|H\rangle_{d4} + |V\rangle_{d1}|V\rangle_{d2}|V\rangle_{d3}|V\rangle_{d4})] \\
 &+ \frac{\alpha\beta}{4}[(|H\rangle_{a1}|H\rangle_{a2}|V\rangle_{a3}|V\rangle_{a4} + |V\rangle_{a1}|V\rangle_{a2}|H\rangle_{a3}|H\rangle_{a4}) \\
 &(|H\rangle_{b1}|H\rangle_{b2}|V\rangle_{b3}|V\rangle_{b4} + |V\rangle_{b1}|V\rangle_{b2}|H\rangle_{b3}|H\rangle_{b4}) \\
 &(|H\rangle_{c1}|H\rangle_{c2}|V\rangle_{c3}|V\rangle_{c4} + |V\rangle_{c1}|V\rangle_{c2}|H\rangle_{c3}|H\rangle_{c4}) \\
 &(|H\rangle_{d1}|H\rangle_{d2}|V\rangle_{d3}|V\rangle_{d4} + |V\rangle_{d1}|V\rangle_{d2}|H\rangle_{d3}|H\rangle_{d4})] \\
 &+ \frac{\alpha^2}{4}[(|H\rangle_{a1}|H\rangle_{a2}|H\rangle_{a3}|H\rangle_{a4} + |V\rangle_{a1}|V\rangle_{a2}|V\rangle_{a3}|V\rangle_{a4}) \\
 &(|H\rangle_{b1}|H\rangle_{b2}|H\rangle_{b3}|H\rangle_{b4} + |V\rangle_{b1}|V\rangle_{b2}|V\rangle_{b3}|V\rangle_{b4}) \\
 &(|H\rangle_{c1}|H\rangle_{c2}|V\rangle_{c3}|V\rangle_{c4} + |V\rangle_{c1}|V\rangle_{c2}|H\rangle_{c3}|H\rangle_{c4}) \\
 &(|H\rangle_{d1}|H\rangle_{d2}|V\rangle_{d3}|V\rangle_{d4} + |V\rangle_{d1}|V\rangle_{d2}|H\rangle_{d3}|H\rangle_{d4})] \\
 &+ \frac{\beta^2}{4}[(|H\rangle_{a1}|H\rangle_{a2}|V\rangle_{a3}|V\rangle_{a4} + |V\rangle_{a1}|V\rangle_{a2}|H\rangle_{a3}|H\rangle_{a4}) \\
 &(|H\rangle_{b1}|H\rangle_{b2}|V\rangle_{b3}|V\rangle_{b4} + |V\rangle_{b1}|V\rangle_{b2}|H\rangle_{b3}|H\rangle_{b4}) \\
 &(|H\rangle_{c1}|H\rangle_{c2}|H\rangle_{c3}|H\rangle_{c4} + |V\rangle_{c1}|V\rangle_{c2}|V\rangle_{c3}|V\rangle_{c4}) \\
 &(|H\rangle_{d1}|H\rangle_{d2}|H\rangle_{d3}|H\rangle_{d4} + |V\rangle_{d1}|V\rangle_{d2}|V\rangle_{d3}|V\rangle_{d4})]. \quad (11)
 \end{aligned}$$

Then, Alice and Bob make the photons in $a1c1$, $a3c3$, $b1d1$, $b3d3$ modes pass through QNDs to make PPC measurements. We find that the PPC results of the items with the coefficient of $\alpha\beta$ are different from the items with the coefficient of α^2 or β^2 . All the PPC results are shown in Table 1, which can be divided into two groups. The left half of table represents the PPC results of the items with the coefficient of $\alpha\beta$. There are 8 possible results, where the photon pairs in $a1c1$ and $a3c3$ ($b1d1$ and $b3d3$) have the same parities. The right half of table represents the PPC results of the items with the coefficients of α^2 or β^2 . There are also 8 possible results, where the photon pairs in $a1c1$ and $a3c3$ ($b1d1$ and $b3d3$) have different parities. For getting the maximally entangled state, we need to select the cases corresponding to the left half of Table 1. In detail, the PPC measurement results of $a1c1$, $a3c3$, $b1d1$,

Table 1 The QND measurement results in the ECP while $m = n = 2$, where “O” is the odd parity, corresponding to the phase shift of $|\alpha\rangle$ is 0 (2θ), “E” is the even parity corresponding to the phase shift of θ .

$\alpha\beta$				α^2 or β^2			
Alice		Bob		Alice		Bob	
a_1c_1	a_3c_3	b_1d_1	b_3d_3	a_1c_1	a_3c_3	b_1d_1	b_3d_3
E	E	E	E	E	O	E	O
		O	O			O	E
O	O	E	E	O	E	E	O
		O	O			O	E

and b_3d_3 are $EEEE$, $EEOO$, $OOEE$, or $OOOO$. For example, if the PPC measurement results are $EEEE$, the state in Eq. (11) will collapse to $|\Phi'\rangle$ as

$$\begin{aligned}
 |\Phi'\rangle = & \frac{1}{\sqrt{2}} \left[\frac{1}{\sqrt{2}} (|H\rangle_{a_1}|H\rangle_{a_2}|H\rangle_{a_3}|H\rangle_{a_4}|H\rangle_{c_1}|H\rangle_{c_2}|H\rangle_{c_3}|H\rangle_{c_4} \right. \\
 & + |V\rangle_{a_1}|V\rangle_{a_2}|V\rangle_{a_3}|V\rangle_{a_4}|V\rangle_{c_1}|V\rangle_{c_2}|V\rangle_{c_3}|V\rangle_{c_4}) \\
 & \frac{1}{\sqrt{2}} (|H\rangle_{b_1}|H\rangle_{b_2}|H\rangle_{b_3}|H\rangle_{b_4}|H\rangle_{d_1}|H\rangle_{d_2}|H\rangle_{d_3}|H\rangle_{d_4} \\
 & + |V\rangle_{b_1}|V\rangle_{b_2}|V\rangle_{b_3}|V\rangle_{b_4}|V\rangle_{d_1}|V\rangle_{d_2}|V\rangle_{d_3}|V\rangle_{d_4}) \\
 & \left. + \frac{1}{\sqrt{2}} \left[\frac{1}{\sqrt{2}} (|H\rangle_{a_1}|H\rangle_{a_2}|V\rangle_{a_3}|V\rangle_{a_4}|H\rangle_{c_1}|H\rangle_{c_2}|V\rangle_{c_3}|V\rangle_{c_4} \right. \right. \\
 & + |V\rangle_{a_1}|V\rangle_{a_2}|H\rangle_{a_3}|H\rangle_{a_4}|V\rangle_{c_1}|V\rangle_{c_2}|H\rangle_{c_3}|H\rangle_{c_4}) \\
 & \frac{1}{\sqrt{2}} (|H\rangle_{b_1}|H\rangle_{b_2}|V\rangle_{b_3}|V\rangle_{b_4}|H\rangle_{d_1}|H\rangle_{d_2}|V\rangle_{d_3}|V\rangle_{d_4} \\
 & \left. + |V\rangle_{b_1}|V\rangle_{b_2}|H\rangle_{b_3}|H\rangle_{b_4}|V\rangle_{d_1}|V\rangle_{d_2}|H\rangle_{d_3}|H\rangle_{d_4}) \right], \quad (12)
 \end{aligned}$$

with a probability of $\frac{1}{2}|\alpha\beta|^2$. Next, Alice and Bob should perform the polarization measurement on the photons in the spatial modes $c_1 - c_4$ and $d_1 - d_4$ in basis of $|\pm\rangle = \frac{1}{\sqrt{2}}(|H\rangle \pm |V\rangle)$. There are sixteen possible measurement results of the photons in $c_1 - c_4$ ($d_1 - d_4$), which are shown in Table 2. As the measurement may change the phase of the items, we divide the sixteen measurement results into four groups. The phases of the items in $a_1a_2a_3a_4$ ($b_1b_2b_3b_4$) modes corresponding to each measurement result group is shown in Table 3. According to Table 2 and Table 3, we can finally determine the state of the photons in $a_1a_2a_3a_4$ ($b_1b_2b_3b_4$). For example, if the measurement results of the photons in both $c_1c_2c_3c_4$ and

Table 2 The sixteen possible measurement results of the photons in modes $c_1 - c_4$ ($d_1 - d_4$) can be divided into four groups, where each group contains four possible results.

Group	1	2	3	4
Results	++++⟩	+--+⟩	+--+⟩	++++⟩
	++--⟩	+--+⟩	+--+⟩	++--⟩
	--++⟩	+--+⟩	+--+⟩	--++⟩
	----⟩	+--+⟩	+--+⟩	----⟩

Table 3 The phases of each items in $a_1a_2a_3a_4$ ($b_1b_2b_3b_4$) corresponding to the measurement results in each group. Here, the subscript $a(b)$ represents $a_1a_2a_3a_4$ ($b_1b_2b_3b_4$).

Items	$ HHHH\rangle_{a(b)}$	$ VVVV\rangle_{a(b)}$	$ HHVV\rangle_{a(b)}$	$ VVHH\rangle_{a(b)}$
1	+	+	+	+
2	+	+	-	-
3	+	-	+	-
4	+	-	-	+

$d_1d_2d_3d_4$ modes belong to group 1 or group 2, the parties will obtain the maximally entangled logic Bell state with the form of

$$\begin{aligned}
 |\Phi'_s\rangle = & \frac{1}{\sqrt{2}} \left[\frac{1}{\sqrt{2}} (|H\rangle_{a_1}|H\rangle_{a_2}|H\rangle_{a_3}|H\rangle_{a_4} \right. \\
 & + |V\rangle_{a_1}|V\rangle_{a_2}|V\rangle_{a_3}|V\rangle_{a_4}) \frac{1}{\sqrt{2}} (|H\rangle_{b_1}|H\rangle_{b_2}|H\rangle_{b_3}|H\rangle_{b_4} \\
 & + |V\rangle_{b_1}|V\rangle_{b_2}|V\rangle_{b_3}|V\rangle_{b_4}) \\
 & \left. + \frac{1}{\sqrt{2}} \left[\frac{1}{\sqrt{2}} (|H\rangle_{a_1}|H\rangle_{a_2}|V\rangle_{a_3}|V\rangle_{a_4} \right. \right. \\
 & + |V\rangle_{a_1}|V\rangle_{a_2}|H\rangle_{a_3}|H\rangle_{a_4}) \frac{1}{\sqrt{2}} (|H\rangle_{b_1}|H\rangle_{b_2}|V\rangle_{b_3}|V\rangle_{b_4} \\
 & \left. + |V\rangle_{b_1}|V\rangle_{b_2}|H\rangle_{b_3}|H\rangle_{b_4}) \right]. \quad (13)
 \end{aligned}$$

On the other hand, if the parties obtain other kinds of measurement results, the parties can not directly obtain the maximally entangled logic Bell state. Fortunately, they can also convert the obtained state to the maximally entangled logic Bell state with the help of the phase-flip operation. Therefore, under the PPC measurement results of $EEEE$, the parties can deterministically obtain the maximally entangled logic Bell state.

In above discussion, we mainly explain the case that the results of QNDs are $EEEE$. If the parties obtain one of the other three cases $EEOO$, $OOEE$, $OOOO$, they can also finally obtain the maximally entangled logic Bell state with the same success probability. Therefore, the total success probability of obtaining the maximally entangled state is $2|\alpha\beta|^2$.

Next we discuss the ECP for a more complicated logic Bell state with $m = 2$ and $n = 3$. The less-entangled logic Bell state can be written as

$$|\bar{\psi}\rangle^{(3,2)} = \alpha|\bar{H}\rangle^{(3,2)}|\bar{H}\rangle^{(3,2)} + \beta|\bar{V}\rangle^{(3,2)}|\bar{V}\rangle^{(3,2)}. \quad (14)$$

Similar to the ECP we discussed above, a pair of initial less-entangled logic Bell states are needed which can be written as

$$\begin{aligned}
 |\bar{\psi}_1\rangle^{(3,2)} = & \alpha|\bar{H}\rangle_a^{(3,2)}|\bar{H}\rangle_b^{(3,2)} + \beta|\bar{V}\rangle_a^{(3,2)}|\bar{V}\rangle_b^{(3,2)} \\
 = & \alpha \left[\frac{1}{2} (|H\rangle_{a_1}|H\rangle_{a_2}|H\rangle_{a_3}|H\rangle_{a_4}|H\rangle_{a_5}|H\rangle_{a_6} \right. \\
 & + |V\rangle_{a_1}|V\rangle_{a_2}|V\rangle_{a_3}|V\rangle_{a_4}|H\rangle_{a_5}|H\rangle_{a_6} \\
 & + |V\rangle_{a_1}|V\rangle_{a_2}|H\rangle_{a_3}|H\rangle_{a_4}|V\rangle_{a_5}|V\rangle_{a_6} \\
 & \left. + |H\rangle_{a_1}|H\rangle_{a_2}|V\rangle_{a_3}|V\rangle_{a_4}|V\rangle_{a_5}|V\rangle_{a_6} \right]
 \end{aligned}$$

$$\begin{aligned}
 & \frac{1}{2} (|H\rangle_{d1}|H\rangle_{d2}|H\rangle_{d3}|H\rangle_{d4}|V\rangle_{d5}|V\rangle_{d6} \\
 & + |H\rangle_{d1}|H\rangle_{d2}|V\rangle_{d3}|V\rangle_{d4}|H\rangle_{d5}|H\rangle_{d6} \\
 & + |V\rangle_{d1}|V\rangle_{d2}|H\rangle_{d3}|H\rangle_{d4}|H\rangle_{d5}|H\rangle_{d6} \\
 & + |V\rangle_{d1}|V\rangle_{d2}|V\rangle_{d3}|V\rangle_{d4}|V\rangle_{d5}|V\rangle_{d6}) \\
 & + \alpha^2 \left[\frac{1}{2} (|H\rangle_{a1}|H\rangle_{a2}|H\rangle_{a3}|H\rangle_{a4}|H\rangle_{a5}|H\rangle_{a6} \right. \\
 & + |V\rangle_{a1}|V\rangle_{a2}|V\rangle_{a3}|V\rangle_{a4}|H\rangle_{a5}|H\rangle_{a6} \\
 & + |V\rangle_{a1}|V\rangle_{a2}|H\rangle_{a3}|H\rangle_{a4}|V\rangle_{a5}|V\rangle_{a6} \\
 & + |H\rangle_{a1}|H\rangle_{a2}|V\rangle_{a3}|V\rangle_{a4}|V\rangle_{a5}|V\rangle_{a6}) \\
 & \frac{1}{2} (|H\rangle_{b1}|H\rangle_{b2}|H\rangle_{b3}|H\rangle_{b4}|H\rangle_{b5}|H\rangle_{b6} \\
 & + |V\rangle_{b1}|V\rangle_{b2}|V\rangle_{b3}|V\rangle_{b4}|H\rangle_{b5}|H\rangle_{b6} \\
 & + |V\rangle_{b1}|V\rangle_{b2}|H\rangle_{b3}|H\rangle_{b4}|V\rangle_{b5}|V\rangle_{b6} \\
 & + |H\rangle_{b1}|H\rangle_{b2}|V\rangle_{b3}|V\rangle_{b4}|V\rangle_{b5}|V\rangle_{b6}) \\
 & \frac{1}{2} (|H\rangle_{c1}|H\rangle_{c2}|H\rangle_{c3}|H\rangle_{c4}|V\rangle_{c5}|V\rangle_{c6} \\
 & + |H\rangle_{c1}|H\rangle_{c2}|V\rangle_{c3}|V\rangle_{c4}|H\rangle_{c5}|H\rangle_{c6} \\
 & + |V\rangle_{c1}|V\rangle_{c2}|H\rangle_{c3}|H\rangle_{c4}|H\rangle_{c5}|H\rangle_{c6} \\
 & + |V\rangle_{c1}|V\rangle_{c2}|V\rangle_{c3}|V\rangle_{c4}|V\rangle_{c5}|V\rangle_{c6}) \\
 & \frac{1}{2} (|H\rangle_{d1}|H\rangle_{d2}|H\rangle_{d3}|H\rangle_{d4}|V\rangle_{d5}|V\rangle_{d6} \\
 & + |H\rangle_{d1}|H\rangle_{d2}|V\rangle_{d3}|V\rangle_{d4}|H\rangle_{d5}|H\rangle_{d6} \\
 & + |V\rangle_{d1}|V\rangle_{d2}|H\rangle_{d3}|H\rangle_{d4}|H\rangle_{d5}|H\rangle_{d6} \\
 & + |V\rangle_{d1}|V\rangle_{d2}|V\rangle_{d3}|V\rangle_{d4}|V\rangle_{d5}|V\rangle_{d6}) \\
 & \left. + \beta^2 \left[\frac{1}{2} (|H\rangle_{a1}|H\rangle_{a2}|H\rangle_{a3}|H\rangle_{a4}|V\rangle_{a5}|V\rangle_{a6} \right. \right. \\
 & + |H\rangle_{a1}|H\rangle_{a2}|V\rangle_{a3}|V\rangle_{a4}|H\rangle_{a5}|H\rangle_{a6} \\
 & + |V\rangle_{a1}|V\rangle_{a2}|H\rangle_{a3}|H\rangle_{a4}|H\rangle_{a5}|H\rangle_{a6} \\
 & + |V\rangle_{a1}|V\rangle_{a2}|V\rangle_{a3}|V\rangle_{a4}|V\rangle_{a5}|V\rangle_{a6}) \\
 & \frac{1}{2} (|H\rangle_{b1}|H\rangle_{b2}|H\rangle_{b3}|H\rangle_{b4}|V\rangle_{b5}|V\rangle_{b6} \\
 & + |H\rangle_{b1}|H\rangle_{b2}|V\rangle_{b3}|V\rangle_{b4}|H\rangle_{b5}|H\rangle_{b6} \\
 & + |V\rangle_{b1}|V\rangle_{b2}|H\rangle_{b3}|H\rangle_{b4}|H\rangle_{b5}|H\rangle_{b6} \\
 & + |V\rangle_{b1}|V\rangle_{b2}|V\rangle_{b3}|V\rangle_{b4}|V\rangle_{b5}|V\rangle_{b6}) \\
 & \frac{1}{2} (|H\rangle_{c1}|H\rangle_{c2}|H\rangle_{c3}|H\rangle_{c4}|H\rangle_{c5}|H\rangle_{c6} \\
 & + |V\rangle_{c1}|V\rangle_{c2}|V\rangle_{c3}|V\rangle_{c4}|H\rangle_{c5}|H\rangle_{c6} \\
 & + |V\rangle_{c1}|V\rangle_{c2}|H\rangle_{c3}|H\rangle_{c4}|V\rangle_{c5}|V\rangle_{c6} \\
 & + |H\rangle_{c1}|H\rangle_{c2}|V\rangle_{c3}|V\rangle_{c4}|V\rangle_{c5}|V\rangle_{c6}) \\
 & \frac{1}{2} (|H\rangle_{d1}|H\rangle_{d2}|H\rangle_{d3}|H\rangle_{d4}|H\rangle_{d5}|H\rangle_{d6} \\
 & + |V\rangle_{d1}|V\rangle_{d2}|V\rangle_{d3}|V\rangle_{d4}|H\rangle_{d5}|H\rangle_{d6} \\
 & + |V\rangle_{d1}|V\rangle_{d2}|H\rangle_{d3}|H\rangle_{d4}|V\rangle_{d5}|V\rangle_{d6} \\
 & \left. + |H\rangle_{d1}|H\rangle_{d2}|V\rangle_{d3}|V\rangle_{d4}|V\rangle_{d5}|V\rangle_{d6}) \right]. \quad (18)
 \end{aligned}$$

The basic principle of the ECP is shown in Fig. 3. Alice and Bob make the photons in spatial modes a_1c_1 , a_3c_3 , a_5c_5 , b_1d_1 , b_3d_3 , b_5d_5 pass through QNDs to make PPC measurements. All possible results of PPC measurements are shown in Table 4, which can be also divided into two groups. The left half of the table represents the PPC mea-

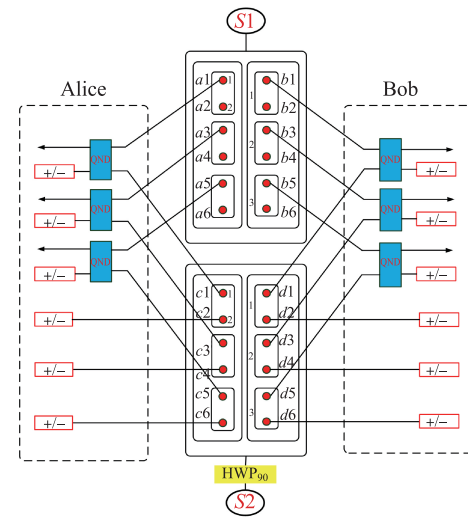


Fig. 3 The schematic drawing of the ECP for logic Bell state with $m = 2$, and $n = 3$. The two big boxes represent two logic Bell states. The two moderate boxes in each big box represent two C-GHZ states. Red dots represent physical qubits.

Table 4 The PPC measurement results for the logic Bell state with $m = 2$, and $n = 3$, where “E” means the even parity and “O” means the odd parity, respectively.

			$\alpha\beta$			α^2 or β^2								
			Alice			Bob			Alice			Bob		
a_1c_1	a_3c_3	a_5c_5	b_1d_1	b_3d_3	b_5d_5	a_1c_1	a_3b_3	a_5c_5	b_1d_1	b_3d_3	b_5d_5			
E	E	E	E	E	E	O	O	O	O	O	O	O	O	O
			O	O	E				E	E	O			
			O	E	O				E	O	E	O	E	
			E	O	O				O	E	E			
O	O	E	E	E	E	E	E	O	O	O	O	O	O	O
			O	O	E				E	E	O			
			O	E	O				E	O	E	O	E	
			E	O	O				O	E	E			
O	E	O	E	E	E	E	O	E	O	O	O	O	O	O
			O	O	E				E	E	O			
			O	E	O				E	O	E	O	E	
			E	O	O				O	E	E			
E	O	O	E	E	E	O	E	E	O	O	O	O	O	O
			O	O	E				E	E	O			
			O	E	O				E	O	E	O	E	
			E	O	O				O	E	E			

surement results of the items with the same coefficient of $\alpha\beta$, where the number of the result E in each of the two parties is odd. They are the successful cases of concentration. The right of the table represents the PPC results of the items with the coefficients of α^2 or β^2 , where the number of the result E in each of the two parties is even. If the parties obtain one of the measurement results in the

right part, the concentration will fail.

We take the successful case corresponding to the mea-

surement results of $EEEEEE$ for example. Under this case, the state in Eq. (18) will collapse to

$$\begin{aligned}
 |\Psi'\rangle = & \frac{1}{\sqrt{2}} \left[\frac{1}{2} (|H\rangle_{a1}|H\rangle_{a2}|H\rangle_{a3}|H\rangle_{a4}|H\rangle_{a5}|H\rangle_{a6}|H\rangle_{c1}|H\rangle_{c2}|H\rangle_{c3}|H\rangle_{c4}|H\rangle_{c5}|H\rangle_{c6} \right. \\
 & + |V\rangle_{a1}|V\rangle_{a2}|V\rangle_{a3}|V\rangle_{a4}|H\rangle_{a5}|H\rangle_{a6}|V\rangle_{c1}|V\rangle_{c2}|V\rangle_{c3}|V\rangle_{c4}|H\rangle_{c5}|H\rangle_{c6} \\
 & + |V\rangle_{a1}|V\rangle_{a2}|H\rangle_{a3}|H\rangle_{a4}|V\rangle_{a5}|V\rangle_{a6}|V\rangle_{c1}|V\rangle_{c2}|H\rangle_{c3}|H\rangle_{c4}|V\rangle_{c5}|V\rangle_{c6} \\
 & + |H\rangle_{a1}|H\rangle_{a2}|V\rangle_{a3}|V\rangle_{a4}|V\rangle_{a5}|V\rangle_{a6}|H\rangle_{c1}|H\rangle_{c2}|V\rangle_{c3}|V\rangle_{c4}|V\rangle_{c5}|V\rangle_{c6}) \\
 & \frac{1}{2} (|H\rangle_{b1}|H\rangle_{b2}|H\rangle_{b3}|H\rangle_{b4}|H\rangle_{b5}|H\rangle_{b6}|H\rangle_{d1}|H\rangle_{d2}|H\rangle_{d3}|H\rangle_{d4}|H\rangle_{d5}|H\rangle_{d6} \\
 & + |V\rangle_{b1}|V\rangle_{b2}|V\rangle_{b3}|V\rangle_{b4}|H\rangle_{b5}|H\rangle_{b6}|V\rangle_{d1}|V\rangle_{d2}|V\rangle_{d3}|V\rangle_{d4}|H\rangle_{d5}|H\rangle_{d6} \\
 & + |V\rangle_{b1}|V\rangle_{b2}|H\rangle_{b3}|H\rangle_{b4}|V\rangle_{b5}|V\rangle_{b6}|V\rangle_{d1}|V\rangle_{d2}|H\rangle_{d3}|H\rangle_{d4}|V\rangle_{d5}|V\rangle_{d6} \\
 & \left. + |H\rangle_{b1}|H\rangle_{b2}|V\rangle_{b3}|V\rangle_{b4}|V\rangle_{b5}|V\rangle_{b6}|H\rangle_{d1}|H\rangle_{d2}|V\rangle_{d3}|V\rangle_{d4}|V\rangle_{d5}|V\rangle_{d6}) \right] \\
 & + \frac{1}{\sqrt{2}} \left[\frac{1}{2} (|H\rangle_{a1}|H\rangle_{a2}|H\rangle_{a3}|H\rangle_{a4}|V\rangle_{a5}|V\rangle_{a6}|H\rangle_{c1}|H\rangle_{c2}|H\rangle_{c3}|H\rangle_{c4}|V\rangle_{c5}|V\rangle_{c6} \right. \\
 & + |H\rangle_{a1}|H\rangle_{a2}|V\rangle_{a3}|V\rangle_{a4}|H\rangle_{a5}|H\rangle_{a6}|H\rangle_{c1}|H\rangle_{c2}|V\rangle_{c3}|V\rangle_{c4}|H\rangle_{c5}|H\rangle_{c6} \\
 & + |V\rangle_{a1}|V\rangle_{a2}|H\rangle_{a3}|H\rangle_{a4}|H\rangle_{a5}|H\rangle_{a6}|V\rangle_{c1}|V\rangle_{c2}|H\rangle_{c3}|H\rangle_{c4}|H\rangle_{c5}|H\rangle_{c6} \\
 & + |V\rangle_{a1}|V\rangle_{a2}|V\rangle_{a3}|V\rangle_{a4}|V\rangle_{a5}|V\rangle_{a6}|V\rangle_{c1}|V\rangle_{c2}|V\rangle_{c3}|V\rangle_{c4}|V\rangle_{c5}|V\rangle_{c6}) \\
 & \frac{1}{2} (|H\rangle_{b1}|H\rangle_{b2}|H\rangle_{b3}|H\rangle_{b4}|V\rangle_{b5}|V\rangle_{b6}|H\rangle_{d1}|H\rangle_{d2}|H\rangle_{d3}|H\rangle_{d4}|V\rangle_{d5}|V\rangle_{d6} \\
 & + |H\rangle_{b1}|H\rangle_{b2}|V\rangle_{b3}|V\rangle_{b4}|H\rangle_{b5}|H\rangle_{b6}|H\rangle_{d1}|H\rangle_{d2}|V\rangle_{d3}|V\rangle_{d4}|H\rangle_{d5}|H\rangle_{d6} \\
 & + |V\rangle_{b1}|V\rangle_{b2}|H\rangle_{b3}|H\rangle_{b4}|H\rangle_{b5}|H\rangle_{b6}|V\rangle_{d1}|V\rangle_{d2}|H\rangle_{d3}|H\rangle_{d4}|H\rangle_{d5}|H\rangle_{d6} \\
 & \left. + |V\rangle_{b1}|V\rangle_{b2}|V\rangle_{b3}|V\rangle_{b4}|V\rangle_{b5}|V\rangle_{b6}|V\rangle_{d1}|V\rangle_{d2}|V\rangle_{d3}|V\rangle_{d4}|V\rangle_{d5}|V\rangle_{d6}) \right], \tag{19}
 \end{aligned}$$

with a probability of $\frac{1}{8}|\alpha\beta|^2$.

The following step is that Alice and Bob measure all the photons in modes $c1 - c6$ and $d1 - d6$ in the basis of $\{|\pm\rangle\}$. Similar with the case corresponding to $m = n = 2$, with the help of the phase-flip operation, the parties can finally obtain the maximally entangled logic Bell state from the state in Eq. (19). In above discussion, we mainly explain the case with the PPC results of $EEEEEE$. If the parties obtain one of the other 15 measurement results in the left half of Table 4, they can also get the maximally entangled logic Bell state with the same principle. In each case, the success probability is $\frac{1}{8}|\alpha\beta|^2$, and the total success probability of obtaining the maximally entangled state is also $2|\alpha\beta|^2$.

It is straightforward to extend this approach to the arbitrary logic Bell state, which means that m and n are arbitrary numbers. As shown in Fig. 4, $S1$ and $S2$ generate two copies of less-entangled logic Bell states $|\varphi_1\rangle^{(n,m)}$ and $|\varphi_2\rangle^{(n,m)}$ as

$$\begin{aligned}
 |\varphi_1\rangle^{(n,m)} &= \alpha|\overline{H}\rangle^{(n,m)}|\overline{H}\rangle^{(n,m)} + \beta|\overline{V}\rangle^{(n,m)}|\overline{V}\rangle^{(n,m)} \\
 &= \alpha \left[\frac{1}{\sqrt{2}} (|GHZ_m^+\rangle^{\otimes n} + |GHZ_m^-\rangle^{\otimes n})_a \right. \\
 & \quad \left. \frac{1}{\sqrt{2}} (|GHZ_m^+\rangle^{\otimes n} + |GHZ_m^-\rangle^{\otimes n})_b \right] \\
 & \quad + \beta \left[\frac{1}{\sqrt{2}} (|GHZ_m^+\rangle^{\otimes n} - |GHZ_m^-\rangle^{\otimes n})_a \right.
 \end{aligned}$$

$$\begin{aligned}
 & \quad \left. \frac{1}{\sqrt{2}} (|GHZ_m^+\rangle^{\otimes n} - |GHZ_m^-\rangle^{\otimes n})_b \right], \tag{20} \\
 |\varphi_2\rangle^{(n,m)} &= \alpha|\overline{H}\rangle^{(n,m)}|\overline{H}\rangle^{(n,m)} + \beta|\overline{V}\rangle^{(n,m)}|\overline{V}\rangle^{(n,m)} \\
 &= \alpha \left[\frac{1}{\sqrt{2}} (|GHZ_m^+\rangle^{\otimes n} + |GHZ_m^-\rangle^{\otimes n})_c \right. \\
 & \quad \left. \frac{1}{\sqrt{2}} (|GHZ_m^+\rangle^{\otimes n} + |GHZ_m^-\rangle^{\otimes n})_d \right] \\
 & \quad + \beta \left[\frac{1}{\sqrt{2}} (|GHZ_m^+\rangle^{\otimes n} - |GHZ_m^-\rangle^{\otimes n})_c \right. \\
 & \quad \left. \frac{1}{\sqrt{2}} (|GHZ_m^+\rangle^{\otimes n} - |GHZ_m^-\rangle^{\otimes n})_d \right]. \tag{21}
 \end{aligned}$$

Then, the parties should perform the bit-flip operation on the photons in modes c and d , which can convert $|\varphi_2\rangle^{(n,m)}$ to $|\varphi_3\rangle^{(n,m)}$ as

$$\begin{aligned}
 |\varphi_3\rangle^{(n,m)} &= \beta|\overline{H}\rangle^{(n,m)}|\overline{H}\rangle^{(n,m)} + \alpha|\overline{V}\rangle^{(n,m)}|\overline{V}\rangle^{(n,m)} \\
 &= \beta \left[\frac{1}{\sqrt{2}} (|GHZ_m^+\rangle^{\otimes n} + |GHZ_m^-\rangle^{\otimes n})_a \right. \\
 & \quad \left. \frac{1}{\sqrt{2}} (|GHZ_m^+\rangle^{\otimes n} + |GHZ_m^-\rangle^{\otimes n})_b \right] \\
 & \quad + \alpha \left[\frac{1}{\sqrt{2}} (|GHZ_m^+\rangle^{\otimes n} - |GHZ_m^-\rangle^{\otimes n})_a \right. \\
 & \quad \left. \frac{1}{\sqrt{2}} (|GHZ_m^+\rangle^{\otimes n} - |GHZ_m^-\rangle^{\otimes n})_b \right]. \tag{22}
 \end{aligned}$$

Next, the parties make the photons in spatial modes $a1c1, a(m+1)c(m+1), a(2m+1)c(2m+1), a(3m+$

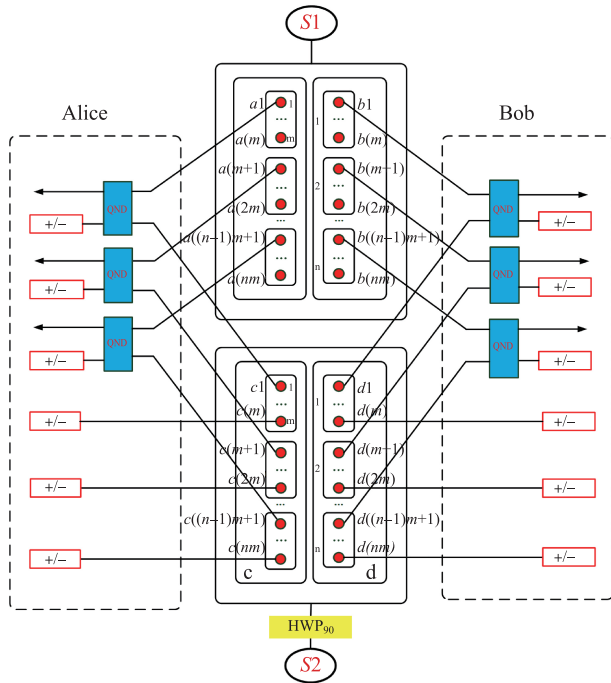


Fig. 4 The schematic drawing of the ECP for logic Bell state with m and n being arbitrary numbers.

$1)c(3m+1), \dots, a((n-1)m+1)c((n-1)m+1)$ and $b1d1, b(m+1)d(m+1), b(2m+1)d(2m+1), b(3m+1)d(3m+1), \dots, b((n-1)m+1)d((n-1)m+1)$ pass through the QNDs to make PPC measurements, and both pick up the items corresponding to the coefficient $\alpha\beta$. Then, they measure all photons in modes $c1 - c(nm)$ and $d1 - d(nm)$ in the basis of $\{|\pm\rangle\}$ and can finally distill the maximally entangled logic Bell state. The total success probability of this arbitrary logic Bell state case is also $2|\alpha\beta|^2$.

4 Discussion

So far, we have completely described our ECP about the logic Bell state. In above section, we only select the items with coefficient $\alpha\beta$, and discard the items with coefficients α^2 and β^2 . Actually, similar to previous ECPs, such discarded items can be reused to distill the maximally entangled logic Bell state, which can increase the success probability of our ECP. We take $m = n = 2$ for example. As shown in Table 1, we consider the case of *EOEO*. With the measurement results of *EOEO*, the state in Eq. (11) will collapse to

$$|\Phi'_f\rangle = \alpha^2 \left[\frac{1}{\sqrt{2}} (|H\rangle_{a1}|H\rangle_{a2}|H\rangle_{a3}|H\rangle_{a4}|H\rangle_{c1}|H\rangle_{c2}|H\rangle_{c3}|H\rangle_{c4} + |V\rangle_{a1}|V\rangle_{a2}|V\rangle_{a3}|V\rangle_{a4}|V\rangle_{c1}|V\rangle_{c2}|V\rangle_{c3}|V\rangle_{c4} \right. \\ \left. \frac{1}{\sqrt{2}} (|H\rangle_{b1}|H\rangle_{b2}|H\rangle_{b3}|H\rangle_{b4}|H\rangle_{d1}|H\rangle_{d2}|H\rangle_{d3}|H\rangle_{d4} + |V\rangle_{b1}|V\rangle_{b2}|V\rangle_{b3}|V\rangle_{b4}|V\rangle_{d1}|V\rangle_{d2}|V\rangle_{d3}|V\rangle_{d4}) \right]$$

$$+\beta^2 \left[\frac{1}{\sqrt{2}} (|H\rangle_{a1}|H\rangle_{a2}|V\rangle_{a3}|V\rangle_{a4}|H\rangle_{c1}|H\rangle_{c2}|V\rangle_{c3}|V\rangle_{c4} + |V\rangle_{a1}|V\rangle_{a2}|H\rangle_{a3}|H\rangle_{a4}|V\rangle_{c1}|V\rangle_{c2}|H\rangle_{c3}|H\rangle_{c4}) \right. \\ \left. \frac{1}{\sqrt{2}} (|H\rangle_{b1}|H\rangle_{b2}|V\rangle_{b3}|V\rangle_{b4}|H\rangle_{d1}|H\rangle_{d2}|V\rangle_{d3}|V\rangle_{d4} + |V\rangle_{b1}|V\rangle_{b2}|H\rangle_{b3}|H\rangle_{b4}|V\rangle_{d1}|V\rangle_{d2}|H\rangle_{d3}|H\rangle_{d4}) \right], \quad (23)$$

with a probability of $\frac{1}{4}(|\alpha|^4 + |\beta|^4)$.

Subsequently, Alice and Bob measure all the photons in modes $c1c2c3c4$ and $d1d2d3d4$ in the basis $|\pm\rangle$, and they can finally obtain the less-entangled logic Bell state as

$$|\Phi''_{f1}\rangle^{(2,2)} = \alpha^2 \left[\frac{1}{\sqrt{2}} (|H\rangle_{a1}|H\rangle_{a2}|H\rangle_{a3}|H\rangle_{a4} + |V\rangle_{a1}|V\rangle_{a2}|V\rangle_{a3}|V\rangle_{a4}) \frac{1}{\sqrt{2}} (|H\rangle_{b1}|H\rangle_{b2}|H\rangle_{b3}|H\rangle_{b4} + |V\rangle_{b1}|V\rangle_{b2}|V\rangle_{b3}|V\rangle_{b4}) \right] \\ + \beta^2 \left[\frac{1}{\sqrt{2}} (|H\rangle_{a1}|H\rangle_{a2}|V\rangle_{a3}|V\rangle_{a4} + |V\rangle_{a1}|V\rangle_{a2}|H\rangle_{a3}|H\rangle_{a4}) \frac{1}{\sqrt{2}} (|H\rangle_{b1}|H\rangle_{b2}|V\rangle_{b3}|V\rangle_{b4} + |V\rangle_{b1}|V\rangle_{b2}|H\rangle_{b3}|H\rangle_{b4}) \right]. \quad (24)$$

Obviously, $|\Phi''_{f1}\rangle^{(2,2)}$ has the similar form as $|\bar{\phi}_1\rangle^{(2,2)}$, and can be reconcentrated in the next round. With the same principle, we can calculate the success probability of the second concentration round as

$$P_2 = 2 \frac{|\alpha|^4 |\beta|^4}{(|\alpha|^2 + |\beta|^2)(|\alpha|^4 + |\beta|^4)}, \quad (25)$$

where the subscript 2 means the second round of concentration. Similarly, we can also calculate the success probability of the k th concentration round as

$$P_k = 2 \frac{|\alpha|^{2k} |\beta|^{2k}}{(|\alpha|^2 + |\beta|^2)(|\alpha|^4 + |\beta|^4) \dots (|\alpha|^{2k} + |\beta|^{2k})}. \quad (26)$$

Therefore, after performing the concentration protocol for k rounds, the total success probability of our ECP is

$$P = P_1 + P_2 + P_3 + \dots + P_k \\ = 2|\alpha|^2 |\beta|^2 + 2 \frac{|\alpha|^4 |\beta|^4}{(|\alpha|^2 + |\beta|^2)(|\alpha|^4 + |\beta|^4)} \\ + 2 \frac{|\alpha|^{2k} |\beta|^{2k}}{(|\alpha|^2 + |\beta|^2)(|\alpha|^4 + |\beta|^4) \dots (|\alpha|^{2k} + |\beta|^{2k})} \\ = \sum_{j=1}^k \frac{2|\alpha|^{2j} |\beta|^{2j}}{\prod_{i=1}^j (|\alpha|^{2i} + |\beta|^{2i})}. \quad (27)$$

In Fig. 5, we calculate the total success probability (P) of this ECP as a function of the entanglement coefficient α . Here, we control the repeating number $k = 1, 2, 3, 4, 5$, respectively. From Fig. 5, we show that when $k = 1$, the total success probability P can only reach the maximum

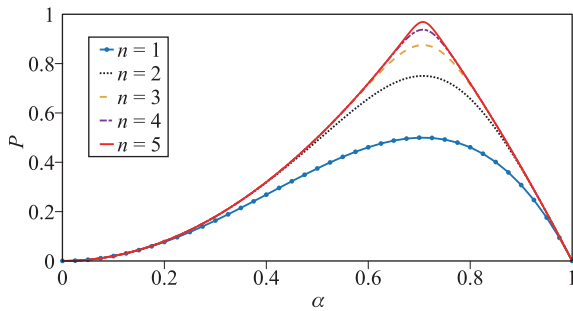


Fig. 5 The total success probability (P) of the ECP as a function of the coefficient α with the iteration number $k = 1, 2, 3, 4, 5$.

of 0.5 when $\alpha = \beta = \frac{1}{\sqrt{2}}$. With the growth of repeating number, the total success probability can be effectively increased. When the repeating number increases to $k = 5$, the maximal value of P will increase to be close to 1.

Finally, let us briefly discuss the cross-Kerr nonlinearity in this protocol. As described above, cross-Kerr nonlinearity plays an important role in many quantum information processing protocols. However, the natural phase shift in a single-photon level is extremely small and it cannot be observed directly [66]. Fortunately, recent experiments showed that the phase shift can be observed in a single-photon level [67, 68]. It opens a door to future potential applications in area of quantum information processing.

5 Conclusion

In conclusion, we propose an efficient entanglement concentration protocol (ECP) for a new kind of logic Bell state, where the logic qubit is the C-GHZ state. In the ECP, we require two pairs of less-entangled logic Bell states. With the help of the nondemolition polarization parity check (PPC) gates constructed with cross-Kerr nonlinearity, we can distill a maximally entangled logic Bell state with some probability. We first explain this ECP for the logic Bell state with $m = n = 2$ and $m = 2$, $n = 3$, respectively. Then, we extend this ECP for the arbitrary logic Bell state. Benefit from the nondemolition PPC gates, the concentrated maximally entangled state can be remained for further applications. Moreover, when the protocol fails, we can repeat the ECP to distill the maximally entangled logic Bell state. By repeating the ECP, the total success probability of our ECP can be effectively increased. This in turn supports the feasibility of our scheme experimentally. Based on the above features, this ECP may have potential applications in long-distance quantum communication in a noisy environment.

Acknowledgements This work was supported by the National Natural Science Foundation of China under Grant Nos. 11474168 and 11747161.

References

1. E. Knill, R. Laflamme, and G. J. Milburn, A scheme for efficient quantum computation with linear optics, *Nature* 409(6816), 46 (2001)
2. C. H. Bennett, G. Brassard, C. Crepeau, R. Jozsa, A. Peres, and W. K. Wootters, Teleporting an unknown quantum state via dual classical and Einstein–Podolsky–Rosen channels, *Phys. Rev. Lett.* 70(13), 1895 (1993)
3. T. C. Li and Z. Q. Yin, Quantum superposition, entanglement, and state teleportation of a microorganism on an electromechanical oscillator, *Sci. Bull.* 61(2), 163 (2016)
4. M. D. G. Ramírez, B. J. Falaye, G. H. Sun, M. Cruz-Irisson, and S. H. Dong, Quantum teleportation and information splitting via four-qubit cluster state and a Bell state, *Front. Phys.* 12(5), 120306 (2017)
5. P. Y. Xiong, X. T. Yu, H. T. Zhan, and Z. C. Zhang, Multiple teleportation via partially entangled GHZ state, *Front. Phys.* 11(4), 110303 (2016)
6. A. K. Ekert, Quantum cryptography based on Bell’s theorem, *Phys. Rev. Lett.* 67(6), 661 (1991)
7. D. Y. Cao, B. H. Liu, Z. Wang, Y. F. Huang, C. F. Li, and G. C. Guo, Multiuser-to-multiuser entanglement distribution based on 1550 nm polarization-entangled photons, *Sci. Bull.* 60(12), 1128 (2015)
8. G. L. Long and X. S. Liu, Theoretically efficient high capacity quantum-key-distribution scheme, *Phys. Rev. A* 65(3), 032302 (2002)
9. F. G. Deng, G. L. Long, and X. S. Liu, Two-step quantum direct communication protocol using the Einstein–Podolsky–Rosen pair block, *Phys. Rev. A* 68(4), 042317 (2003)
10. C. Wang, F. G. Deng, Y. S. Li, X. S. Liu, and G. L. Long, Quantum secure direct communication with high dimension quantum superdense coding, *Phys. Rev. A* 71(4), 044305 (2005)
11. J. Y. Hu, B. Yu, M. Y. Jing, L. T. Xiao, S. T. Jia, G. Q. Qin, and G. L. Long, Experimental quantum secure direct communication with single photons, *Light Sci. Appl.* 5(9), e16144 (2016)
12. W. Zhang, D. S. Ding, Y. B. Sheng, L. Zhou, B. S. Shi, and G. C. Guo, Quantum secure direct communication with quantum memory, *Phys. Rev. Lett.* 118(22), 220501 (2017)
13. F. Zhu, W. Zhang, Y. B. Sheng, and Y. D. Huang, Experimental long-distance quantum secret direct communication, *Sci. Bull.* 62(22), 1519 (2017)
14. Y. B. Sheng and L. Zhou, Distributed secure quantum machine learning, *Sci. Bull.* 62(14), 1025 (2017)
15. X. Q. Shao, T. Y. Zheng, and S. Zhang, Engineering steady three-atom singlet states via quantum-jump based feedback, *Phys. Rev. A* 85(4), 042308 (2012)
16. X. Q. Shao, T. Y. Zheng, C. H. Oh, and S. Zhang, Dissipative creation of three-dimensional entangled state in optical cavity via spontaneous emission, *Phys. Rev. A* 89(1), 012319 (2014)

17. X. Q. Shao, J. B. You, T. Y. Zheng, C. H. Oh, and S. Zhang, Stationary three-dimensional entanglement via dissipative Rydberg pumping, *Phys. Rev. A* 89(5), 052313 (2014)
18. T. Y. Ye, Robust quantum dialogue based on a shared auxiliary logical Bell state against collective noise, *Sci. China Phys. Mech. Astron.* 58, 040301 (2015)
19. W. Huang, Q. Su, B. J. Xu, B. Liu, F. Fan, H. Y. Jia, and Y. H. Yang, Improved multiparty quantum key agreement in travelling mode, *Sci. China Phys. Mech. Astron.* 59(12), 120311 (2016)
20. C. J. Liu, W. Ye, W. D. Zhou, H. L. Zhang, J. H. Huang, and L. Y. Hu, Entanglement of coherent superposition of photon-subtraction squeezed vacuum, *Front. Phys.* 12(5), 120307 (2017)
21. M. Y. Wang, F. L. Yan, and T. Gao, Generation of four photon polarization entangled decoherence-free states with cross-Kerr nonlinearity, *Sci. Rep.* 6(1), 38233 (2016)
22. A. Farouk, J. Batle, M. Elhoseny, M. Naseri, M. Lone, A. Fedorov, M. Alkhambashi, S. H. Ahmed, and M. Abdel-Aty, Robust general N user authentication scheme in a centralized quantum communication network via generalized GHZ states, *Front. Phys.* 13(2), 130306 (2018)
23. J. Batle, A. Farouk, O. Tarawneh, and S. Abdalla, Multipartite quantum correlations among atoms in QED cavities, *Front. Phys.* 13(1), 130305 (2018)
24. C. H. Bennett, G. Brassard, S. Popescu, B. Schumacher, J. A. Smolin, and W. K. Wootters, Purification of noisy entanglement and faithful teleportation via noisy channels, *Phys. Rev. Lett.* 76(5), 722 (1996)
25. W. Dür, H. J. Briegel, J. I. Cirac, and P. Zoller, Quantum repeaters based on entanglement purification, *Phys. Rev. A* 59(1), 169 (1999)
26. J. W. Pan, C. Simon, Č. Brukner, and A. Zeilinger, Entanglement purification for quantum communication, *Nature* 410(6832), 1067 (2001)
27. D. Gonça and P. van Loock, High-fidelity entanglement purification using chains of atoms and optical cavities, *Phys. Rev. A* 86(5), 052312 (2012)
28. M. Zwerger, H. J. Briegel, and W. Dür, Universal and optimal error thresholds for measurement-based entanglement purification, *Phys. Rev. Lett.* 110(26), 260503 (2013)
29. M. Zwerger, H. J. Briegel, and W. Dür, Robustness of hashing protocols for entanglement purification, *Phys. Rev. A* 90(1), 012314 (2014)
30. J. Z. Bernád, J. M. Torres, L. Kunz, and G. Alber, Multiphoton-state-assisted entanglement purification of material qubits, *Phys. Rev. A* 93(3), 032317 (2016)
31. C. H. Bennett, H. J. Bernstein, S. Popescu, and B. Schumacher, Concentrating partial entanglement by local operations, *Phys. Rev. A* 53(4), 2046 (1996)
32. S. Bose, V. Vedral, and P. L. Knight, Purification via entanglement swapping and conserved entanglement, *Phys. Rev. A* 60(1), 194 (1999)
33. T. Yamamoto, M. Koashi, and N. Imoto, Concentration and purification scheme for two partially entangled photon pairs, *Phys. Rev. A* 64(1), 012304 (2001)
34. Z. Zhao, J. W. Pan, and M. S. Zhan, Practical scheme for entanglement concentration, *Phys. Rev. A* 64(1), 014301 (2001)
35. Y. B. Sheng, L. Zhou, S. M. Zhao, and B. Y. Zheng, Efficient single-photon-assisted entanglement concentration for partially entangled photon pairs, *Phys. Rev. A* 85(1), 012307 (2012)
36. F. G. Deng, Optimal nonlocal multipartite entanglement concentration based on projection measurements, *Phys. Rev. A* 85(2), 022311 (2012)
37. Y. B. Sheng, L. Zhou, and S. M. Zhao, Efficient two-step entanglement concentration for arbitrary W states, *Phys. Rev. A* 85(4), 042302 (2012)
38. Z. H. Peng, J. Zou, X. J. Liu, Y. J. Xiao, and L. M. Kuang, Atomic and photonic entanglement concentration via photonic Faraday rotation, *Phys. Rev. A* 86(3), 034305 (2012)
39. C. Cao, C. Wang, L. Y. He, and R. Zhang, Atomic entanglement purification and concentration using coherent state input-output process in low- Q cavity QED regime, *Opt. Express* 21(4), 4093 (2013)
40. Y. B. Sheng, J. Pan, R. Guo, L. Zhou, and L. Wang, Efficient N -particle W state concentration with different parity check gates, *Sci. China Phys. Mech. Astron.* 58(6), 060301 (2015)
41. M. Y. Wang, F. L. Yan, and J. Z. Xu, Perfect entanglement concentration of an arbitrary four-photon polarization entangled state via quantum nondemolition detectors, *J. Phys. B-At. Mol. Opt.* 49(15), 155502 (2016)
42. C. C. Qu, L. Zhou, and Y. B. Sheng, Entanglement concentration for concatenated Greenberger–Horne–Zeilinger state, *Quantum Inform. Process* 14(11), 4131 (2015)
43. J. Pan, L. Zhou, S. P. Gu, X. F. Wang, Y. B. Sheng, and Q. Wang, Efficient entanglement concentration for concatenated Greenberger–Horne–Zeilinger state with the cross-Kerr nonlinearity, *Quantum Inform. Process* 15(4), 1669 (2016)
44. A. M. Steane and B. Ibinson, Fault-tolerant logical gate networks for Calderbank–Shor–Steane codes, *Phys. Rev. A* 72(5), 052335 (2005)
45. S. Muralidharan, C. L. Zou, L. S. Li, J. M. Wen, and L. Jiang, Overcoming erasure errors with multilevel systems, *New J. Phys.* 19(1), 013026 (2017)
46. F. Fröwis and W. Dür, Stable macroscopic quantum superpositions, *Phys. Rev. Lett.* 106(11), 110402 (2011)
47. H. Lu, L. K. Chen, C. Liu, P. Xu, X.C. Yao, L. Li, N.L. Liu, B. Zhao, Y.A. Chen, and J.W. Pan, Experimental realization of a concatenated Greenberger–Horne–Zeilinger state for macroscopic quantum superpositions, *Nat. Photonics* 8(5), 364 (2014)
48. F. Fröwis and W. Dür, Stability of encoded macroscopic quantum superpositions, *Phys. Rev. A* 85(5), 052329 (2012)

49. F. Kesting, F. Fröwis, and W. Dür, Effective noise channels for encoded quantum systems, *Phys. Rev. A* 88(4), 042305 (2013)
50. D. Ding, F. L. Yan, and T. Gao, Preparation of kmphoton concatenated Greenberger–Horne–Zeilinger states for observing distinctive quantum effects at macroscopic scales, *JOSA B* 30(11), 3075 (2013)
51. L. Zhou and Y. B. Sheng, Complete logic Bell-state analysis assisted with photonic Faraday rotation, *Phys. Rev. A* 92(4), 042314 (2015)
52. Y. B. Sheng and L. Zhou, Two-step complete polarization logic Bell-state analysis, *Sci. Rep.* 5(1), 13453 (2015)
53. L. Zhou and Y. B. Sheng, Feasible logic Bell-state analysis with linear optics, *Sci. Rep.* 6(1), 20901 (2016)
54. T. C. Ralph, A. J. F. Hayes, and A. Gilchrist, Loss-tolerant optical qubits, *Phys. Rev. Lett.* 95(10), 100501 (2005)
55. A. Gilchrist, A. J. F. Hayes, and T. C. Ralph, Efficient parity-encoded optical quantum computing, *Phys. Rev. A* 75(5), 052328 (2007)
56. J. Borregaard, A. S. Sørensen, J. I. Cirac, and M. D. Lukin, Efficient quantum computation in a network with probabilistic gates and logical encoding, *Phys. Rev. A* 95(4), 042312 (2017)
57. S. Muralidharan, J. Kim, N. Lütkenhaus, M. D. Lukin, and L. Jiang, Ultrafast and fault-tolerant quantum communication across long distances, *Phys. Rev. Lett.* 112(25), 250501 (2014)
58. F. Ewert, M. Bergmann, and P. van Loock, Ultrafast long-distance quantum communication with static linear optics, *Phys. Rev. Lett.* 117(21), 210501 (2016)
59. K. Nemoto and W. J. Munro, Nearly deterministic linear optical controlled-not gate, *Phys. Rev. Lett.* 93(25), 250502 (2004)
60. B. He, Q. Lin, and C. Simon, Cross-Kerr nonlinearity between continuous-mode coherent states and single photons, *Phys. Rev. A* 83(5), 053826 (2011)
61. Y. Q. He, D. Ding, F. L. Yan, and T. Gao, Exploration of photon-number entangled states using weak nonlinearities, *Opt. Express* 23(17), 21671 (2015)
62. X. M. Xiu, Q. Y. Li, Y. F. Lin, H. K. Dong, L. Dong, and Y. J. Gao, Preparation of four-photon polarization entangled decoherence-free states employing weak cross-Kerr nonlinearities, *Phys. Rev. A* 94(4), 042321 (2016)
63. L. Dong, Y. F. Yin, C. Cui, H. K. Dong, X. M. Xiu, and Y. J. Gao, Fault-tolerant distribution of GHZ states and controlled DSQC based on parity analyses, *Opt. Express* 25(16), 18581 (2017)
64. L. Dong, J. X. Wang, Q. Y. Li, H. Z. Shen, H. K. Dong, X. M. Xiu, and Y. J. Gao, Single logical qubit information encoding scheme with the minimal optical decoherence free subsystem, *Opt. Lett.* 41(5), 1030 (2016)
65. L. Dong, Y. F. Lin, Q. Y. Li, H. K. Dong, X. M. Xiu, and Y. J. Gao, Generation of three-photon polarization entangled decoherence-free states, *Ann. Phys.* 371, 287 (2016)
66. P. Kok, W. J. Munro, K. Nemoto, T. C. Ralph, J. P. Dowling, and G. J. Milburn, Linear optical quantum computing with photonic qubits, *Rev. Mod. Phys.* 79(1), 135 (2007)
67. G. Kirchmair, B. Vlastakis, Z. Leghtas, S. E. Nigg, H. Paik, E. Ginossar, M. Mirrahimi, L. Frunzio, S. M. Girvin, and R. J. Schoelkopf, Observation of quantum state collapse and revival due to the single-photon Kerr effect, *Nature* 495(7440), 205 (2013)
68. A. Feizpour, M. Hallaji, G. Dmochowski, and A. M. Steinberg, Observation of the nonlinear phase shift due to single post-selected photons, *Nat. Phys.* 11(11), 905 (2015)